A. Brömme, C. Busch, A. Dantcheva, C. Rathgeb and A. Uhl (Eds.): BIOSIG 2017,
Lecture Notes in Informatics (LNI), Gesellschaft für Informatik, Bonn 2017 71

xTARP: Improving the Tented Arch Reference Point Detection Algorithm

Johannes Merkle[1], Benjamin Tams[2], Benjamin Dieckmann[3], Ulrike Korte[4]

Abstract: In 2013, Tams et al. proposed a method to determine directed reference points in fingerprints based on a mathematical model of typical orientation fields of tented arch type fingerprints. Although this *Tented Arch Reference Point* (TARP) method has been used successfully for pre-alignment in biometric cryptosystems, its accuracy does not yet ensure satisfactory error rates for single finger systems.

In this paper, we improve the TARP algorithm by deploying an improved orientation field computation and by integrating an additional mathematical model for arch type fingerprints. The resulting *Extended Tented Arch Reference Point* (xTARP) method combines the arch model with the tented arch model and achieves a significantly better accuracy than the original TARP algorithm. When deploying the xTARP method in the Fuzzy Vault construction of Butt et al., the false non-match rate (FNMR) at a security level of 20 bits is reduced from 7.4% to 1.7%.

Keywords: Fingerprint Registration, Reference Point Detection, Biometric Template Protection.

1 Introduction

Reliable reference point detection is an important building block for identification systems and biometric cryptosystems based on fingerprint minutiae. With the help of a reference point, an absolute pre-alignment can be applied for fingerprint registration, thereby compensating variations in the placement (translation) and, if constituted with a direction, rotation of different imprints from the same finger.

The most prominent reference points are the singular points of the orientation field, i.e. core and delta points. Many algorithms for singular point detection have been proposed, e.g. [ZHY01, BG02, NB03]. However, fingerprints of type *arch* do not have any singular points and, therefore, singular point detection alone is not a universal approach. Many publications proposed algorithms for the estimation of generalized singular points, e.g., highest curvature points, that are also present in arch-type fingerprints, e.g. [Ja00, RA00, LJK05, Ig06, GZY16]. An alternative approach is the estimation of a so-called *focal point* [ASJ06, AB08, BA09]. However, most of these universal methods (exceptions being [LJK05] and [BA09]) do not output a direction which could be used to compensate different rotations of the fingerprints.

[1] secunet Security Networks, Mergenthaler Allee 77, Eschborn, Germany, johannes.merkle@secunet.com
[2] secunet Security Networks, Konrad-Zuse-Platz 2, München, Germany, benjamin.tams@secunet.com
[3] secunet Security Networks, Mergenthaler Allee 77, Eschborn, Germany, benjamin.dieckmann@secunet.com
[4] Bundesamt für Sicherheit in der Informationstechnik, Bonn, Germany, ulrike.korte@bsi.bund.de

A promising approach to determine directed reference points was published in [Ta13] and [TMM15]. There, the actual fingerprint's orientation field is aligned with a mathematical orientation field model for fingerprints of type *tented arch*.[5] The alignment between the orientation field of the fingerprint and the orientation field of the mathematical model results from a minimization of a cost function measuring the deviation between these fields in a region around the model's core point. In [Ta13, TMM15, Bu16, Ta16, Ta15], this *Tented Arch Reference Point* (TARP) algorithm was successfully applied in biometric cryptosystems based on the *fuzzy vault scheme*. However, the achieved error rates were still too high for practical applications, which indicates that the TARP algorithm is not yet sufficiently accurate.

We improve the TARP algorithm by several means. Firstly, we integrate an improved orientation field computation. Furthermore, we implement an additional mathematical model for arch-type fingerprints and develop a fusion method to make use of both models. As a result, we obtain an *Extended Tented Arch Reference Point* (xTARP) algorithm which exhibits a considerably higher accuracy than the TARP and other reference point estimation methods. We show the utility of our xTARP algorithm by deploying it for pre-alignment in the Fuzzy Vault construction of [Bu16] (instead of the TARP algorithm).

The structure of this paper is as follows. We give a brief introduction into the TARP method in Section 2 and analyze its potential for improvement in Section 3. In Section 4, we describe our improvements. The resulting xTARP algorithm is evaluated and compared with other methods for singular point detection in Section 5. Finally, we draw conclusions in Section 6.

2 The Tented Arch Reference Point Algorithm

The Tented Arch Reference Point (TARP) algorithm for estimating directed reference points was proposed in [Ta13] and (with slightly improved parameters) in [TMM15] and its implementation in C++ was published under LGPLv3 license.[6]

Fig. 1: For most fingerprints, the ridge flow around the center resembles that of a fingerprint of type tented arch.

[5] Note, that this tented arch model is applied to fingerprints of all types
[6] http://www.stochastik.math.uni-goettingen.de/biometrics/thimble

The basic idea of the TARP algorithm is that, for most fingerprints, the ridge flow in a ring-shaped area around the center resembles that of a fingerprint of type *tented arch*, as illustrated in Figure 1. Therefore, the TARP algorithm attempts to align the orientation field of the fingerprint to a fixed directional field resembling the orientation field of fingerprints of type tented arch. The directional field is derived from a modification of the the *quadratic differential* (QD) model [HHM08], which represents fingerprint orientation fields of arch-type fingerprints by the complex function

$$\psi(z) = \lambda^2(z^2 - R^2), \tag{1}$$

with $\mathrm{Im}(z) > 0$ and real-valued parameters λ, R. The orientation at location (a,b) is defined by $\phi = 0.5\mathrm{Arg}(\psi(a+i\cdot b))$. For fingerprints of type *tented arch*, the model is extended to $\tau(z) = \psi(z)\frac{z^2+d_{\mathrm{core}}^2}{z^2+d_{\mathrm{delta}}^2}$, where $(0,d_{\mathrm{core}})$ and $(0,d_{\mathrm{delta}})$ with $d_{\mathrm{core}} \geq d_{\mathrm{delta}} \geq 0$ are the positions of the core and delta point, respectively, in the model. We refer to [HHM08] for further details and explanations.

By setting $\tau_{\alpha,\beta}(z) = \alpha^{-2}\tau(\alpha z + \beta)$, the TARP algorithm applies translations β and rotations α (with $\alpha, \beta \in \mathbb{C}$ and $|\alpha| = 1$)[7] to the tented arch model $\tau(z)$ to find the best fit with the fingerprint orientation field in a region around the model's core point. In this translated and rotated model, the core point's position is $\gamma_{\alpha,\beta} = \alpha^{-1}(i\cdot d_{\mathrm{core}} - \beta)$. If the fingerprint's orientation field is given by $\{(z_j, v_j)\}$, where the z_j are quantized positions and v_j the orientation at position z_j, its fit with the model $\tau_{\alpha,\beta}(z)$ is evaluated using the cost function

$$\kappa(\alpha,\beta) = \sum_j w_{\alpha,\beta}(z_j)\left|\frac{\tau_{\alpha,\beta}(z_j)}{|\tau_{\alpha,\beta}(z_j)|} - v_j\right|; \tag{2}$$

here, $w_{\alpha,\beta}(z) = \exp\left(-\frac{(|z-\gamma_{\alpha,\beta}-\rho|)^2}{2\sigma^2}\right)$ is a weight function resulting from a Gaussian function with deviation σ rotated at distance ρ around the core $\gamma_{\alpha,\beta}$. [8] The reference point is defined as the core point $\gamma_{\alpha,\beta}$ for those α,β that minimize the cost function; its direction is given by the model's rotation $\mathrm{Arg}(\alpha)$.

In order to minimize the cost function (2) over α and β, a two-step approach is performed. In an initial search step, for all positions in a rectangular grid of width g and for $\alpha = 0$, the corresponding translation β is computed and the cost function $\kappa(\alpha,\beta)$ is evaluated. Starting with the value (α,β) from the initial search resulting in the smallest $\kappa(\alpha,\beta)$, a steepest descent algorithm is performed in which the cost function is further minimized. In the steepest descent, the rotation α and the translation β are refined alternatively, until the value of $\kappa(\alpha,\beta)$ converges to a (local) minimum. If the steepest descent does not result in a reference point inside the fingerprint's foreground, it is repeated starting with the next best candidate from the initial search. The iteration continues until a reference point on the fingerprint's foreground is found or the steepest descent has failed $n_{\max}$ times.

[7] Recall that when representing numbers in the complex plane, addition translates to vector addition and multiplication results in addition of the arguments (angles) and multiplication of the absolute values (lengths).

[8] The distance ρ of the Gaussian function's center from the core point results in a ring-like shape (with smooth borders) of the weight function so that the region directly at the core point, where the orientation field computation is often unreliable, is less weighted.

A visualization of the TARP model and its parameters can be found in [TMM15]. In [TMM15], the parameters $\lambda = 1.81, d_{\text{core}} = 160, d_{\text{delta}} = 22, R = 175, \rho = 45, \sigma = 12, g = 7$ and $n_{\max} = 20$ were chosen based on a training on the FVC2000 DB2b database comprising 80 fingerprints.

3 Analysis of the Improvement Potential

We identified the following potential sources of inaccuracies of the TARP algorithm.

- **Segmentation.** The TARP algorithm performs segmentation by a combination of Otsu thresholding [LO79] and Graham scan [Gr72]. This relatively simple approach sometimes fails, e.g., when the imprints of the first and the second finger pad are not clearly separated.
- **Orientation field.** The TARP algorithm computes orientation fields by local intensity gradients without any post-processing. Therefore, errors in the orientation fields may contribute considerably to the inaccuracies of the reference point detection.
- **Model.** As visible in Figure 1, the tented arch model fits well for most types of fingerprints but not that good for arch-type fingerprints.
- **Minimization.** The steepest descent (gradient) method may yield merely a local (but not global) minimum of the cost function.

In order to focus our effort to improve the TARP algorithm on those aspects that promise the highest gain in accuracy, we analyzed the impact of each of these factors to the accuracy of the reference points. For that purpose, we manually marked ground truth data for the segmentation and orientation fields of 273 optical sensor fingerprints of right index fingers from the MCYT database [Or03] for which the TARP algorithm showed relatively poor performance. Furthermore, we modified the TARP algorithm so that it can be fed with externally generated segmentation maps and orientation fields. Then, we computed the reference points for these fingerprints with and without the ground truth segmentation maps and/or orientation fields and evaluated the accuracy of the alignments resulting from these reference points, using the metric described in Section 5. In order to investigate the third factor, we manually determined the type of all imprints of right index fingers of the MCYT database and, for each type, evaluated the accuracy of the alignments resulting from the reference points computed with the TARP algorithm. Furthermore, we modified the TARP implementation so that the minimum of the cost function is determined by exhaustive search, and evaluated the accuracy in comparison to the original method (steepest descent).

The results in Figure 2 clearly show that the errors in the computation of orientation fields has much more impact on the accuracy than incorrect segmentation, and that the TARP algorithm performs much worse on arch-type fingerprints than on other types of fingerprints. Compared to these factors, the minimization of the cost function showed slightly less potential for improvement. Therefore, we decided to improve the TARP algorithm by deploying a better orientation field computation method and by extending the tented arch model to arch type fingerprints.

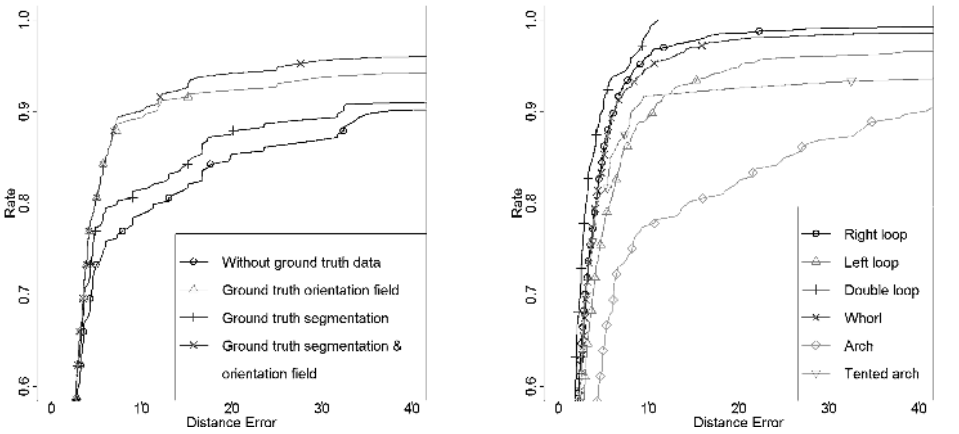

Fig. 2: Evaluation of the dependence of the accuracy of the TARP algorithm on errors in segmentation and/or orientation field computation (left hand side) and on the type of fingerprint. The diagrams show the ECDF of distance errors on two different sets of fingerprints from the MCYT database.

4 Improvements

4.1 Improved Orientation Field Computation

In order to improve the orientation field computation, we deployed the algorithm described in [LP08], which applies a Markov Random Field to improve the initial orientation field obtained by a gradient approach. The Markov Random Field is constructed from two components: a component based on a global mixture model obtained from training on real fingerprints and a component enforcing pairwise consistency of neighboring image blocks. We used an implementation of this algorithm contained in the FingerJetFX open source minutiae extractor[9].

In [TMM15], the parameters of the TARP method were chosen based on a training on the FVC2000 DB2b database comprising 80 fingerprints. Since this training set was quite small and the improved orientation field computation may favor different parameters, we conducted a new training on a large training set comprising 2736 fingerprints of 228 right index fingers from the MCYT database [Or03]. Precisely, we deployed the TARP algorithm in the Fuzzy Vault implementation of [Bu16] and evaluated the FNMR for a degree $k = 6$ of the secret polynomials (which gives approximately 20 bits of security). We found the highest accuracy for $\lambda = 1.3, d_{\text{core}} = 340, d_{\text{delta}} = 32, R = 185, \rho = 28, \sigma = 6$. The best trade-off between accuracy and processing time was found for $g = 7$ and $n_{\max} = 5$. Note that the parameters $d_{\text{core}}, d_{\text{delta}}, R, \rho, \sigma, g$ apply for 500 dpi images and need to be linearly scaled for other resolutions.

[9] https://github.com/FingerJetFXOSE/FingerJetFXOSE

4.2 Developing a Modified Algorithm for Arches (ARP)

Furthermore, we designed and implemented an Arch Reference Point (ARP) detection algorithm based on the quadratic differential model $\psi(z)$ for arch-type fingerprints specified in (1). Analogously to the TARP algorithm, it tries to find a translation $\beta \in \mathbb{C}$ and a rotation $\alpha \in \mathbb{C}$ (with $|\alpha| = 1$) so that the correspondingly transformed model $\psi_{\alpha,\beta}(z) = \alpha^{-2}\psi(\alpha z + \beta)$, fits best with the fingerprint's actual orientation field in the area around a reference point. In the original model $\psi(z)$, this reference point is set to $(0,d)$, and after transformation by α,β its position is $\overline{\gamma}_{\alpha,\beta} = \alpha^{-1}(i \cdot d - \beta)$. The fit of the fingerprint's orientation field $\{(z_j, v_j)\}$ with the model $\psi_{\alpha,\beta}(z)$ is evaluated using a cost function

$$\overline{\kappa}(\alpha,\beta) = \sum_j \overline{w}_{\alpha,\beta}(z_j) \left| \frac{\psi_{\alpha,\beta}(z_j)}{|\psi_{\alpha,\beta}(z_j)|} - v_j \right|, \tag{3}$$

where $\overline{w}_{\alpha,\beta}(z) = \exp\left(-\frac{(|z-\overline{\gamma}_{\alpha,\beta}|)^2}{2\sigma^2}\right)$ is a weight function resulting from a two-dimensional Gaussian function with deviation σ and center $\overline{\gamma}_{\alpha,\beta}$. [10] A visualization of both the ARP model and the weight function is shown in Figure 3.

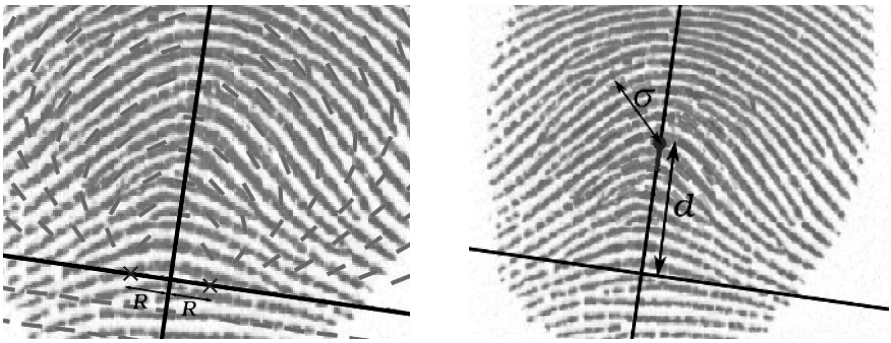

(a) (b)

Fig. 3: Visualization of the ARP model (a) and the weight function (b) and the corresponding parameters. The parameter λ is not visualized; it controls how stretched the ARP model is.

For the minimization of the cost function (3) over α and β, the same two-step method as in the TARP algorithm, i.e. an initial search over a rectangular grid of width g followed by a steepest descent (see Section 2), is applied, using the parameters $m, r, \alpha_{\max}$ (width of the grid, number of rotations and maximum rotation angle used in the initial search) and $n_{\max}$ (maximum number of attempts for the steepest descent). After minimizing $\overline{\kappa}(\alpha,\beta)$ over α,β, the algorithm outputs the reference point $\overline{\gamma}_{\alpha,\beta}$ with orientation $\mathrm{Arg}(\alpha)$.

Analogously to the training of the improved TARP method, we optimized the parameters of the ARP algorithm by deploying it in the Fuzzy Vault implementation of [Bu16] and

[10] The weight function $\overline{w}_{\alpha,\beta}$ has its maximum at the reference point, in contrast to the weight function $w_{\alpha,\beta}$ used in the TARP model, which has its maximum on a circle with radius ρ around the core point. (see Footnote 8)

evaluating the false reject rate (FRR) at $k = 6$ for a training set of 393 arch-type fingerprints (captured with an optical sensor) of 33 left and right index fingers from the MCYT database [Or03]. The best recognition accuracy was achieved for $\lambda = 1.5, d = 80, R = 20, \sigma = 27, g = 5, n_{\max} = 5$. Analogously to the parameters of the TARP method, the values of the parameters d, R, σ, g apply for 500 dpi images and need to be linearly scaled for other resolutions.

4.3 Implementing xTARP by Fusion of TARP and ARP

In order to combine TARP and ARP in an Extended Tented Arch Reference Point (xTARP) method, we needed a rule to decide which of the two points to choose. We could have tried to use a classifier to detect arch-type fingerprints, but as it turned out in our evaluation, the ARP method works well not only on this fingerprint class. Since the minimized values κ and $\overline{\kappa}$ of the cost functions (2) and (3) of the TARP and the ARP algorithm, respectively, indicate how good the fingerprint's orientation field fits with the respective QD model, we decided to implement a classifier using the values κ and $\overline{\kappa}$ as input. For a training set of 4920 fingerprints of 410 left and right index fingers from the MCYT database [Or03], we computed reference points with both algorithms and used these for pre-alignment in the Fuzzy Vault implementation of [Bu16]. Then, we selected as training classes two subsets of fingerprints, for which one of the two methods (TARP or ARP, respectively) yields less than 8 genuine points in the unlocking set but the other method results in at least 8 genuine points.

Since a genuine comparison will already yield a poor result if one of the two reference points is inaccurate, the larger one of the cost function values of the reference and the query fingerprint should be more indicative for the genuine score than the lower one. Therefore, as input data for the training we computed, for each genuine pair, the maximum $\kappa_{\max} = \max(\kappa_{\text{ref}}, \kappa_{\text{que}})$ of the TARP cost values of reference and query fingerprint and, analogously, the maximum $\overline{\kappa}_{\max} = \max(\overline{\kappa}_{\text{ref}}, \overline{\kappa}_{\text{que}})$ of both cost values of the ARP algorithm. For the two classes and the input vector $(\kappa_{\max}^{[i]}, \overline{\kappa}_{\max}^{[i]})$ we optimized a linear discriminant function, starting with logistic regression and optimizing the coefficients by evaluating the resulting FRR of the Fuzzy Vault with $k = 6$ for the complete training set. We obtained the best results for the linear discriminant function $y = 0.6 \cdot \overline{\kappa} - \kappa + 10$, i.e., when selecting the ARP point if and only if $\kappa > 0.6 \cdot \overline{\kappa} + 10$. This classification rule was implemented into our xTARP algorithm. We also investigated classifiers based on support vector machines with various kernels but did not obtain significantly better results.

5 Experiments

We performed experiments to evaluate the accuracy of the xTARP algorithm and to compare it with the original TARP algorithm from [TMM15] and other methods for reference point detection.

Since the ARP and TARP reference points cannot be visually identified by humans, like core or delta points, we cannot measure the accuracy of the reference points with respect to ground-truth data. In order to overcome this problem and to allow a fair comparison with other publications, we compute, for each finger, an approximation of the "true reference point" by means of the median of the computed reference points. Precisely, for each fingerprint, we manually determined the affine transformations (rotation and translation) by which it is aligned with the other fingerprints of the same finger.[11] Using these transformations, we projected the reference points of the other fingerprints into this fingerprint. From all projected reference points (with accordingly rotated orientations) and the reference point of this finger, we computed the median of the positions and orientations as approximated "true reference point".

For a reference point (x, y, θ), we measured the distance error *DE* as the Euclidean distance to the approximated "true reference point" $(\bar{x}, \bar{y}, \bar{\theta})$ of the fingerprint, i.e. as $DE = \sqrt{(x-\bar{x})^2 + (y-\bar{y})^2}$, and the rotation error *RE* as the absolute value of the smaller angle (in degrees) between their directions, i.e. as $RE = \min(\delta_\theta, 360 - \delta_\theta)$, where δ_θ is the representative of $(\theta - \bar{\theta})$ mod 360 in the interval $[0, 360)$.

5.1 Evaluation of Optimizations

First, we evaluated the effectiveness of our improvements by comparing the accuracy of our xTARP algorithm and the original TARP method from [TMM15]. For this evaluation, we used as a test set the optical sensor fingerprints of right index fingers of the first 100 subjects in the MCYT database [Or03]. This test set is disjoint to the training sets used for optimization of parameters and fusion (Section 4), and it comprises 1200 fingerprints (12 per finger) of relatively high quality taken with the sensor *UareU* from Digital Persona at 500 dpi and stored in uncompressed image files of 256×400 pixels. The results show that both distance errors and rotation errors are considerably reduced (Figure 4).

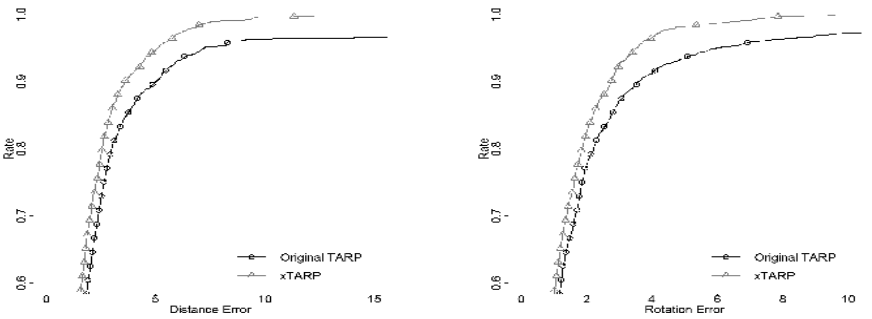

(a) (b)

Fig. 4: ECDF of distance errors (a) and rotation errors (b) of the original TARP method (black) and our xTARP algorithm (red).

[11] In cases where non-linear distortions did not allow an accurate global alignment, we chose a transformation that aligns the central region of the finger pad where the reference points are expected to be located.

Whereas the original TARP algorithm fails (i.e., does not find a reference point) for 0.5% of the images, the xTARP algorithm processes all of them successfully. The optimized TARP algorithm (as described in Section 2) already achieves error rates close to that of the xTARP method, but it fails for 0.67% of the images.

5.2 Comparison with Other Approaches

In order to compare our xTARP algorithm with other methods for reference point detection, we evaluated it on FVC2000 DB2a as well. This data base comprises 800 fingerprints from right index fingers of 100 subjects (8 per finger), acquired by a low cost capacitive sensor at 500 dpi and stored in image files with loss-less compression and 256×364 pixels.

Table 1 compares the accuracy of the xTARP method[12] with other state-of-the-art methods for reference point detection. Note, that the methods of [LJK05, Ig06, AB08, GZY16] do not determine any orientation of the reference point (indicated by "n.a.").

Method	$DE < 5$	$DE < 10$	$DE < 20$	$RE < 5$	$RE < 11.25$	$RE < 22.5$	Fail
xTARP	612	734	763	610	752	790	5
[GZY16]	569	719	784	n.a.	n.a.	n.a.	0
[BA09]	n.a.	668	769	n.a.	521	657	0
[AB08]	285	640	763	n.a.	n.a.	n.a.	1
[Ig06]	n.a.	712	753	n.a.	n.a.	n.a.	0
[LZH06]	n.a.	654	745	n.a.	690	737	9
[LJK05]	n.a.	659	749	n.a.	n.a.	n.a.	13

Tab. 1: Cumulative statistics of the distance errors (DE), rotation errors (RE), and number of failures (no reference point is output) of our xTARP method and other reference point detection methods. An entry "n.a." means that the corresponding value is not provided in the referenced publications or (in the case of RE) that the method does not compute any orientation of the reference point.

As shown in Table 1, the xTARP method outperforms all other methods with respect to distance errors for up to 10 pixels. Furthermore, xTARP is by far the most accurate method with respect to rotation errors.

On the other hand, our improvements of the TARP algorithm are much less effective for the FVC2000 DB2a database as they are for the MCYT database, i.e., the original TARP method already exhibits a similar accuracy as the xTARP method. The reasons of this finding are yet to be analyzed.

5.3 Application in a Fuzzy Vault for Fingerprints

In order to prove the utility of the xTARP method, we applied it for the pre-alignment of the fingerprints in the Fuzzy Vault construction of [Bu16]. Precisely, we deployed the

[12] Based on a training on the FVC 2000 DB2a, we slightly adapted the linear discriminant function for the fusion (see Section 4.3).

variant which uses minutiae's positions and orientations but not their type and applied the same parameters as in [Bu16] for the degree k of the (monic) secret polynomial from 5 to 8. Our evaluation shows that the false match rate (FMR) does not depend on the pre-alignment method, which is quite plausible because the concept of an exact alignment does not make sense for impostor verifications. Therefore, the estimates from [Bu16] for the security level and FMR also apply for an alignment with our improved methods.

Due to the fusion of two different models (ARP and TARP) by the xTARP method, it can happen that a different model is used for the reference fingerprint as for the query fingerprint. Such an inconsistent application of the models almost always results in a non-match, because the location of TARP and ARP points are typically different. To overcome this problem, we store a status bit with the reference template, indicating which of the two methods were used during enrolment, and use the same method for verification. By this approach, we operate the xTARP method in a *stateful mode*, in contrast to the *stateless mode*, where the decision between ARP and TARP is taken for each fingerprint independently. Another advantage of the stateful mode is that only one reference point is computed for the query fingerprint and, thus, the processing time of the verification is reduced. For the stateful mode, we found a slightly different linear discriminant function $y = 0.8 \cdot \overline{\kappa} - \kappa - 28$ to be optimal for fusion (see Section 4.3).

For the various stages of development of the xTARP method, we evaluated the FNMR[13] on the same test set as in [Bu16] (right index fingers of the first 100 subjects of the MCYT data base). The results in Table 2 show that the FNMR is already greatly reduced for the TARP method with the improved orientation field estimation, and even further by the xTARP method. For the xTARP method, the storage of a status bit along the template indicating whether a TARP or an ARP reference point has been used for enrolment (stateful mode) further improves the error rates.

	Method	$k=5$	$k=6$	$k=7$	$k=8$
FNMR	Original TARP	6.0%	7.4%	9.6%	13.1%
	Improved TARP	1.6%	2.8%	4.8%	7.6%
	ARP	2.0%	3.5%	5.9%	9.6%
	xTARP (stateless)	0.5%	1.7%	3.8%	6.6%
	xTARP (stateful)	0.5%	1.5%	3.4%	6.3%
FMR	all	1.9%	0.3%	0.04%	0%
Security (bits)	all	16.5	20	24	27

Tab. 2: Error rates of the Fuzzy Vault construction of [Bu16] when using different variants of the xTARP and TARP method for pre-alignment.

The FNMR can be even further reduced to 0.2%, 0.8%, 2.2% and 4.6%, respectively, if during verification, in case of a non-match, a second attempt is conducted with a reference point computed with the orientation field estimation from the original TARP algorithm.

[13] In this Fuzzy Vault construction, failures of the reference point detection also contribute to the FNMR.

6 Conclusions

We have greatly improved the accuracy of the TARP reference point detection method by deploying a better algorithm for orientation field estimation and by complementing the tented arch model with a model for plain arches. When using the resulting xTARP method in a biometric cryptosystem, the FNMR for a security level of 20 bits drops from 7% to 1.7%.

Nevertheless, we still see significant potential for further improvements: the xTARP algorithm tends to be inaccurate for fingerprints where the true reference point is close to the edge of the foreground, which is often the case for the FVC2000 DB2a data base. In these regions, the cost function is partially evaluated on the background, where the orientations are constant or randomly chosen (we tried both options without obtaining significantly different results), which increases the cost value and may imply that the minimum is found in a different region. Therefore, we suspect that a better performance can be achieved by limiting the cost function to the foreground. However, for the deepest descent method to work, the cost function has to be smooth.

Furthermore, due to the combination of two different fingerprint models, the computational effort is quite large and should be improved. Currently, the xTARP algorithm takes more than 1.5 seconds in stateless mode and 0.7 seconds in stateful mode. Since the algorithm has not been optimized yet with respect to computational complexity, we believe that there is great potential to tab. For instance, the computation of the cost function is based on convolution and, thus, could be considerably sped up using Fast Fourier Transformation.

References

[AB08] Areekul, Vutipong; Boonchaiseree, Natthawat: Fast focal point localization algorithm for fingerprint registration. In: Industrial Electronics and Applications, 2008. ICIEA 2008. 3rd IEEE Conference on. IEEE, pp. 2089–2094, 2008.

[ASJ06] Areekul, Vutipong; Suppasriwasuseth, Kittiwat; Jirachawang, Suksan: The New Focal Point Localization Algorithm for Fingerprint Registration. In: 18th International Conference on Pattern Recognition (ICPR 2006), 20-24 August 2006, Hong Kong, China. pp. 497–500, 2006.

[BA09] Boonchaiseree, Natthawat; Areekul, Vutipong: Focal Point Detection Based on Half Concentric Lens Model for Singular Point Extraction in Fingerprint. In: Advances in Biometrics, Third International Conference, ICB 2009, Alghero, Italy, June 2-5, 2009. Proceedings. pp. 637–646, 2009.

[BG02] Bazen, Asker M.; Gerez, Sabih H.: Systematic Methods for the Computation of the Directional Fields and Singular Points of Fingerprints. IEEE Trans. Pattern Anal. Mach. Intell., 24(7):905–919, 2002.

[Bu16] Butt, Moazzam et al.: Correlation-resistant fuzzy vault for fingerprints. In: Proc. of Sicherheit 2016. volume 256 of LNI. GI, pp. 125–136, 2016.

[Gr72] Graham, Ronald L.: An Efficient Algorithm for Determining the Convex Hull of a Finite Planar Set. Inf. Process. Lett., 1(4):132–133, 1972.

[GZY16] Guo, Xifeng; Zhu, En; Yin, Jianping: A fast and accurate method for detecting fingerprint reference point. Neural Computing and Applications, pp. 1–11, 2016.

[HHM08] Huckemann, Stephan; Hotz, Thomas; Munk, Axel: Global Models for the Orientation Field of Fingerprints: An Approach Based on Quadratic Differentials. IEEE Trans. Pattern Anal. Mach. Intell., 30(9):1507–1519, 2008.

[Ig06] Ignatenko, Tanya et al.: Reference point detection for improved fingerprint matching. In: Security, Steganography, and Watermarking of Multimedia Contents VIII, San Jose, CA, USA, January 15, 2006. p. 60720G, 2006.

[Ja00] Jain, Anil K. et al.: Filterbank-based fingerprint matching. IEEE Trans. Image Processing, 9(5):846–859, 2000.

[LJK05] Liu, Manhua; Jiang, Xudong; Kot, Alex ChiChung: Fingerprint Reference-Point Detection. EURASIP J. Adv. Sig. Proc., 2005(4):498–509, 2005.

[LO79] Level Otsu, N: A threshold selection method from gray-level histogram. IEEE Transactions on Systems, Man and Cybernetics, 9(1):62–66, 1979.

[LP08] Lee, Kuang-chih; Prabhakar, Salil: Probabilistic orientation field estimation for fingerprint enhancement and verification. In: Biometrics Symposium, 2008. BSYM'08. IEEE, pp. 41–46, 2008.

[LZH06] Liu, Tong; Zhang, Chao; Hao, Pengwei: Fingerprint Reference Point Detection Based on Local Axial Symmetry. In: 18th International Conference on Pattern Recognition (ICPR 2006), 20-24 August 2006, Hong Kong, China. pp. 1050–1053, 2006.

[NB03] Nilsson, Kenneth; Bigün, Josef: Localization of corresponding points in fingerprints by complex filtering. Pattern Recognition Letters, 24(13):2135–2144, 2003.

[Or03] Ortega-Garcia, J. et al.: MCYT baseline corpus: a bimodal biometric database. IEE Proc. on Vision, Image and Signal Processing, 150(6):395–401, 2003.

[RA00] Rerkrai, Krisakorn; Areekul, Vutipong: A New Reference Point for Fingerprint Recognition. In: Proceedings of the 2000 International Conference on Image Processing, ICIP 2000, Vancouver, BC, Canada, September 10-13, 2000. pp. 499–502, 2000.

[Ta13] Tams, Benjamin: Absolute Fingerprint Pre-Alignment in Minutiae-Based Cryptosystems. In: Proc. of BIOSIG 2013. volume 212 of LNI. GI, pp. 75–86, 2013.

[Ta15] Tams, Benjamin et al.: Improved Fuzzy Vault Scheme for Alignment-Free Fingerprint Features. In: Proc. of BIOSIG 2015. volume 245 of LNI. GI, 2015.

[Ta16] Tams, Benjamin: Unlinkable minutiae-based fuzzy vault for multiple fingerprints. IET Biometrics, 5(3):170–180, 2016.

[TMM15] Tams, B.; Mihăilescu, P.; Munk, A.: Security Considerations in Minutiae-based Fuzzy Vaults. IEEE Trans. Inf. Forensics Security, 10(5):985–998, 2015.

[ZHY01] Zhang, Qinzhi; Huang, Kai; Yan, Hong: Fingerprint Classification Based on Extraction and Analysis of Singularities and Pseudoridges. In: Visualisation 2001, Selected Papers from the Pan-Sydney Area Workshop on Visual Information Processing, VIP2001. pp. 83–87, 2001.